RESEARCH ARTICLE | JULY 03 2019

A correlation between electron-hole pair radii and magnetomodulation of exciplex fluorescence in electron donor-electron acceptor organic systems

Daniel Pelczarski; Piotr Grygiel; Karol Falkowski; Waldemar Stampor

Appl. Phys. Lett. 115, 013301 (2019)
https://doi.org/10.1063/1.5095878

Applied Physics Letters ARTICLE scitation.org/journal/apl

A correlation between electron-hole pair radii and magnetomodulation of exciplex fluorescence in electron donor-electron acceptor organic systems

Cite as: Appl. Phys. Lett. **115**, 013301 (2019); doi: 10.1063/1.5095878
Submitted: 13 March 2019 · Accepted: 7 June 2019 ·
Published Online: 3 July 2019

Daniel Pelczarski, Piotr Grygiel,[a] Karol Falkowski, and Waldemar Stampor

AFFILIATIONS

Department of Physics of Electronic Phenomena, Gdańsk University of Technology, Gdańsk 80-233, Poland

[a]Electronic mail: piotr.grygiel@pg.edu.pl

ABSTRACT

Electric field dependencies of electromodulated photoluminescence and magnitudes of the magnetic-field effect on photoluminescence have been measured in vacuum-evaporated films of m-MTDATA [4, 4′, 4″-tris(N-(3-methylphenyl)-N-phenylamino)triphenylamine]:bathophenanthroline, m-MTDATA:BCP (bathocuproine), as well as 4, 4′, 4″-tris[2-naphthyl(phenyl)amino]triphenylamine:BCP. The Sano-Tachiya-Noolandi-Hong extension of standard Onsager formalism was used to investigate the electron-hole pair dissociation process which allowed us to estimate the pair intercarrier distances and the final speed of carrier recombination. A distinct correlation between the pair radii and the magnitude of the magnetic-field effect has been found.

It is generally recognized that the efficiency of organic electroluminescence (EL) diodes and photovoltaic (PV) devices is limited mainly by the recombination of charge carriers and dissociation of excitons, which are usually assumed to proceed via the intermediate stage of the finite-lifetime electron-hole (e-h) pair.[18] Among other parameters, the e-h pair (EHP) intercarrier distance should be a subject of interest for addressing the issue whether the same pairs are involved in the dissociation/recombination processes, as well as for modeling the exciton dissociation to optimize the efficiency of the EL and PV devices.

A useful tool for probing the radius of spin-correlated e-h pairs is the investigation of the magnetic field effect on photoluminescence (MPL) of relevant organic systems. The mechanisms of such an influence are the subject of intensive studies, and for the case of the external magnetic field on the hyperfine milliteslas scale, the e-h pair (EHP) model has been applied.[10,14,17,27] Accordingly, under the external magnetic field, the intersystem crossing (ISC) between the singlet, ^{1}(e-h), triplet, ^{3}(e-h), and pair spin states becomes weaker due to the Zeeman splitting of the triplet ones. Therefore, if the pair spin-coherence time is sufficiently long, the singlet-triplet splitting becomes strong enough for e-h pairs of short radius to block the ISC. Since the electrostatic exchange interactions do decrease exponentially with carrier separation, in the case of quasidegenerated singlet and triplet states, when the pair radius is long enough, the ISC becomes more effective. Here, the mechanism of pair conversion is related to the precession of magnetic dipoles of electrons in the hyperfine magnetic field of protons.[11] Thus, the external magnetic field can modulate the effectiveness of various channels of the e-h pair decay, i.e., the production of emissive states in EL devices (or charge carriers in PV ones). Within the EHP model, a correlation between the pair intercarrier distance and the magnitude of the magnetic-field effect on photoluminescence of a proper organic system should then be observed.

In our correlation study, the vacuum-evaporated, two-component films of the 1:1 mass ratio mixtures with the electron donor, D (of lower ionization potential), and acceptor, A (with larger electron affinity), were investigated. It is generally recognized that in such systems, the emitting (fluorescent, FL) intermolecular excited-state complexes (exciplex states), $(DA)^*$, are created following the photoinduced electron transfer between neighboring D and A molecules, i.e., excited encounter complexes.[3,22] This transfer proceeds over an intrapair distance, r_0, with probability η_0, the latter assumed to be independent of external electric field strength (hereafter denoted by F) and yields the geminate e-h pairs, $^1(D^+ \ldots A^-)$. The $^1(D^+ \ldots A^-)$ pairs can in turn dissociate while escaping the Coulombic attraction of the countercharges to produce the free D^+ and A^- charge carriers with escape probability, $\Omega(F)$, which increases with F. The exciplex states are formed due to

the alternative process of intermediate pair recombination, with the probability of $1-\Omega(F)$. Note that the $(DA)^*$ states can also be generated without the involvement of geminate pairs, i.e., directly from the encounter complexes, which has been suggested by Weller.[28] The population of FL states is then sensitive to F and a significant electromodulation of exciplex photoluminescence (PL) intensity, I, should be observed in proper D:A systems, according to the formula

$$I(F) = \frac{k_f}{k_f + k_n}\left[1 - \eta_0\Omega(F)\right]I^*. \quad (1)$$

Here, k_f and k_n stand for the rate constants of the radiative and nonradiative pathways of exciplex decay and I^* is the production rate of optically excited encounter complexes. Henceforth, the analysis of the electromodulated photoluminescence (EML) measurements on D:A mixtures provides an effective tool for determining the values of the e-h pair final recombination speed and the distance at which the final recombination occurs. For this purpose, the EML experimental data are to be reproduced with the use of appropriate theoretical curves.[9]

To describe the recombination process, Onsager[23] formalism regarding the Brownian random walk of $^1(D^+\ldots A^-)$ geminate e-h pairs in a continuous medium is commonly used, however, with (somehow unrealistic) assumption of the process infinite velocity at point centers, i.e., with zero-separation between electrons and holes. Although considered as a relatively less effort-consuming method for rationalization of the e-h pair dissociation, the approach does not allow us to determine the carrier recombination rate and recombination distance. This is, however, possible using an extension of the Onsager theory as developed by Sano and Tachiya[25] and, independently, by Noolandi and Hong[21] (hereafter STNH), where the nonzero e-h distance and the finite kinetic rate of final recombination events can be extracted at the cost of quite tedious mathematical operations. The averaged escape probability, $\Omega(F)$, is calculated by integration of the product of the escape probability (depending on the approach chosen) and a function representing the initial distribution of pair separations assumed here to be isotropic and given by a Dirac delta function.

In the EML experiments, the optically excited photoluminescence of an organic layer sandwiched between semitransparent electrodes is quenched by the applied electric field sinusoidally varying with time, $F(t) = F_0 \sin \omega t$. The sample response is observed at the second harmonic, 2ω, of the fundamental frequency, ω, using the phase-sensitive (lock-in) detection device (typically here at $\omega/2\pi = 175$ Hz). The EML signal is measured as a function of the rms electric field strength, F_{rms}, and is defined by (see Ref. 16 for technique details)

$$(2\omega)\mathrm{EML} = \frac{I_{2\omega}}{I_{0\omega}}, \quad (2)$$

where $I_{2\omega}$ denotes the rms value of the second-order and $I_{0\omega}$ is the steady state Fourier component of the sample PL intensity, $I(t) = \sum I_{n,\omega}(t)$, $n = 0, 1, 2, \ldots$. Note that the electric-field induced PL quenching is indicated here by the presence of the positive values of the $I_{0\omega}$ and $I_{2\omega}$ components (also see Ref. 9). Importantly, the EML technique provides a more direct insight into the electric field influence on the recombination/dissociation processes as compared to the photocurrent measurements. This is because the EML outcomes are not affected by, e.g., the field dependence of carrier trapping and mobility and by optical injection of charge at the sample electrodes. Some care is, however, generally advised when interpreting the EML data since they may be altered by some other physical factors. This issue has been discussed in our previous paper[24] in the context of one of the D:A systems used in the present study. Particularly, the parasite PL electromodulation can occur due to quenching interactions between excitons or free/trapped charge carriers. Nevertheless, for significant quenching, the effective introduction of the latter into the organic system is required, i.e., due to the bulk photogeneration or efficient injection/ejection by the electrode/material interface. This is, however, not the case of samples with poor-injecting electrodes and when the strong (of 10% or more) PL reduction is observed. The exciton quenching on (of relatively high concentration) trapped carriers is in turn acceptably reduced by utilizing the AC voltage to modulate F. Next, the external electric field can modify the electronic energy transfer which is expected in materials with molecules of rather large permanent dipole moments, not used in our experiments. Similarly, the observation of the EML signal as originating from the global spectrum of the sample PL eliminates the results of the Stark effect, i.e., the shift of the corresponding energy levels by the external electric field as interacting with permanent and induced molecular dipoles. Furthermore, for given organic systems, the EML sample responses do not follow the F^2 function which is expected with the Stark effect involved and tend to saturate in a range of high F, exceeding ca. 8×10^5 V/cm. Moreover, the electroabsorption signals that reflect the Stark shifts are usually at least several times smaller than the EML signals which are obtained for materials investigated here for the same wavelengths of absorbed light. The presence of the Stark effect may also be expected to influence the lifetime of emissive states due to F-induced modulation of rate constants of the internal conversion (IC), the ISC process, as well as the electron transfer between the D- and A-part of a molecule. Nevertheless, the corresponding reduction of the PL intensity has been determined to be of several parts of a percent for a variety of organic compounds under electric field strengths used in our measurements. Therefore, such effects can safely be omitted as compared with the PL quenching reported in the present paper, being always of a 10% order or more. As the electric-field characteristics of the (2ω)EML signal in the present paper are well-correlated with the photocurrent ones (see Ref. 24), we shall state that the e-h pair dissociation channel plays a dominant role in PL quenching in investigated photoconductive compounds, with its sensitivity to F overwhelming the effect of the possible electric-field-enhanced, highly photoinduced intermolecular electron transfer (PIET) discussed widely in the literature.

In the MPL measurements, the photoluminescent sample is influenced by a magnetic field (being here parallel to the layer surface) and consists of a DC- and AC-component, with the latter varying sinusoidally with time, $B(t) = B_{DC} + B_0 \sin \omega t$ (at $\omega/2\pi$ between 0.5 and 2 Hz being the lowest applicable for the phase-sensitive detection system used due to weak and noisy sample responses). The magnitude of the MPL signal is here determined by the ratio

$$\mathrm{MPL} = \frac{I(B) - I(0)}{I(0)}, \quad (3)$$

where $I(B)$ and $I(0)$ are the photoluminescence intensities in the presence and the absence of the magnetic field, respectively. The MPL curves are obtained by numerical integration, $I(B) - I(0) = \int_{B_{DC=0}}^{B_{DC}} dI$ with the use of differentiation by the modulation method, $dI = (\partial I/\partial B_{DC})\Delta B_{DC}$. It is worth noting that, according to our former

considerations,[24] both the long-radius $^1(D^+\ldots A^-)_{long}$ and short-radius $^1(D^+\ldots A^-)_{short}$ pairs can be generated from relevant encounter complexes in low-dielectric-constant D:A systems. Importantly, prevailingly, the $^1(D^+\ldots A^-)_{long}$ pairs are those that could dissociate to generate free charge carriers (forming the sample photocurrent) or, via the ISC process, produce the triplet, $^3(D^+\ldots A^-)_{long}$, ones. These triplet pairs practically do not contribute to the photoconductivity in systems with efficient none-radiative decay to the ground state via low-energy molecular triplets (so-called "triplet drain").[4] As the $^1(D^+\ldots A)_{long}$ pairs do mainly recombine nonradiatively, their operation cannot be optically detected when applying the external magnetic field to the photoconducting sample. On the other hand, since the ISC transition, $^1(D^+\ldots A^-)_{short} \rightarrow {}^3(D^+\ldots A^-)_{short}$, is rather ineffective due to larger singlet-triplet splitting, the magnetic field, by suppressing the ISC $^1(D^+\ldots A^-)_{short} \rightarrow {}^3(D^+\ldots A^-)_{short}$ transition, gives only a minor rise to the population of $^1(D^+\ldots A^-)_{short}$ pairs. Hence, a positive weak magnetic field-effect on sample PL should be observed.

As electron donors in the D:A systems, we have utilized two amine-derivatives: 4, 4′, 4″-tris(N-(3-methylphenyl)-N-phenylamino)-triphenylamine (m-MTDATA) and 4, 4′, 4″-tris[2-naphthyl(phenyl)-amino] triphenylamine (2TNATA), with acceptors such as bathophenanthroline (BPhen) and bathocuproine (BCP). The fact that the exciplex states are involved in the emission process of these mixtures can be recognized from the relevant parts of Fig. 1. Accordingly, the structureless, broad-banded PL spectra of coevaporated layers being ascribed to the emission of exciplexes, are clearly shifted toward the red as compared to the FL ones of each of the system monomer components. Note that such kinds of compounds are used as light emitters in the EL diodes[12] and that m-MTDATA and BCP have been utilized as the A- and D-compounds for the construction of a bifunctional PV/EL device with expectations of good performance applications.[5] The vacuum-evaporated quartz/D:A[1:1] structures and the quartz/Al/D:A[1:1]/Al sandwich ones were used for the MPL and EML measurements, respectively.

Now, consider the electric field characteristics for the global FL (2ω)EML signal according to definition (2) as reproduced by the Onsager- and STNH-approach. The relevant analytical expressions for $\Omega(F)$ as well as the numerical procedures used for the calculations can be found in Ref. 9. In both models, the value of the initial e-h pair radius, r_0/r_C, and in the STNH approach, the recombination sphere radius, a/r_C, together with the carrier capture velocity parameter, $\kappa r_C/D$, were individually set for each D:A mixture for the best fitting results. Here, D is the relative diffusion coefficient ($D = D_e + D_h$) and $r_C = e^2/4\pi\varepsilon_0\varepsilon_r k_B T$ is the Onsager (Coulombic capture) radius, with e being the elementary charge, $\varepsilon_0\varepsilon_r$ being the electric permittivity of the medium, k_B being the Boltzmann constant, and T being the absolute temperature. Note that $r_C = 187$ Å for $\varepsilon_r = 3.0$ and $T = 298$ K which is equal to many intermolecular distances in relevant organic solids. In the corresponding parts of Fig. 2, the experimental (2ω)EML outcomes are marked by squares, the best-fit Onsager curves are plotted by a solid lines, whereas those for the STNH approach are plotted by the broken ones.

As far as the set of data for all donor-acceptor systems is considered, both theoretical approaches generally follow fairly well the (2ω)EML signal. Some minor discrepancies, however, are observed in the case of 2TNATA:BCP in the range of low electric fields. From the outcomes obtained for m-MTDATA:BCP (taken from our former paper[24]), one can see the stronger and stronger deviation of the Onsager curve with increasing F_{rms}. In addition, the performance of the STNH model gradually fails for higher values of F_{rms} at the lowest value of $\kappa r_C/D$ as can be seen for m-MTDATA:BPhen from Fig. 2(c). The values of the a-recombination distance higher than $0.05r_C$ result in rather poor quality of fitting [see Fig. 2(b)]. For the sake of comparison, the optimal values of the $\kappa r_C/D$ ratio together with those of the calculated recombination sphere radius, a, and initial e-h pair intercarrier distances for all the investigated systems are collected in Table I. As shown, in all cases, the same value of a (approximately equal to an average intermolecular distance in a crystal lattice) results from the fitting procedures but, importantly, different intercarrier distances, r_0 (as high as 2–3 intermolecular distances), are obtained. Taking into account the typical (hole) mobility $\mu = 1 \times 10^{-5}$ cm^2/V s, from the Einstein relation, $D = \mu k_B T/e$, one gets $D = 2.6 \times 10^{-7}$ cm^2/s. Therefore, for the investigated systems, we get the final recombination speed $(0.01 < \kappa < 14)$ cm/s, with this parameter being rarely reported in the literature. It is worth noting that $\kappa = 1$ cm/s translates into the recombination lifetime $\tau \approx a/\kappa \approx 100$ ns comparing well with the experimental PL decay time in the m-MTDATA:BPhen system of 200 ns.[13] This in turn indicates the substantial contribution of the exciplex formation process to the apparent PL lifetime since the ionic pathway of exciplex formation prevails in the investigated systems ($\eta_0 \approx 0.8 - 0.9$ in m-MTDATA and 0.3 in 2TNATA systems).

The geminate e-h pair dissociation/recombination processes in PV (e.g., Refs. 8 and 19; also see Ref. 18) and EL (e.g., Ref. 15) organic devices with charge transfer (CT)/exciplex exited states have usually been characterized in terms of the (purely empirical) Braun model.[2]

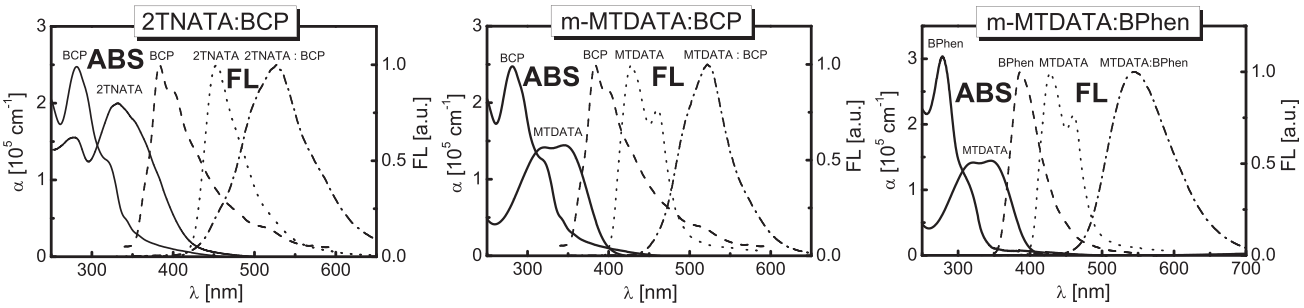

FIG. 1. Absorption (ABS—solid lines) and fluorescence (FL—broken lines) spectra of the monomers and donor-acceptor systems.

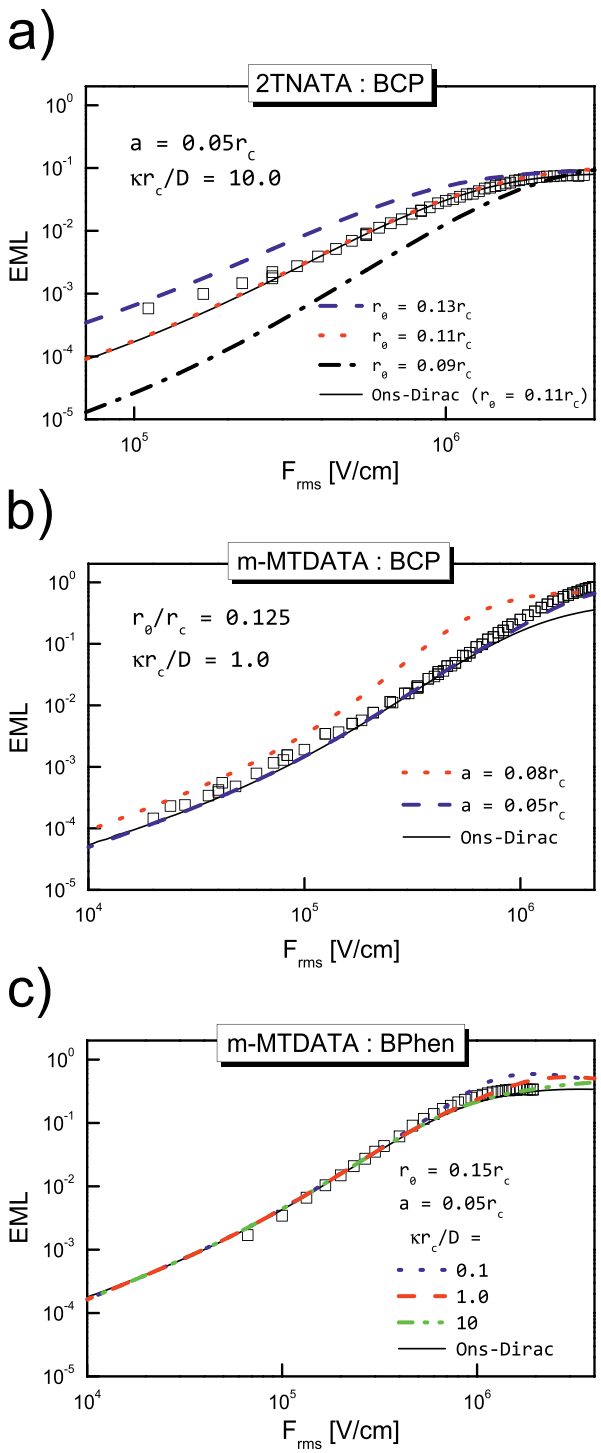

FIG. 2. The electric field dependencies of the global (2ω)EML signal for three donor-acceptor systems. The squares are for the EML measurements, the solid line stands for the best-fit according to the Onsager formalism, and the broken ones—for the STNH approach. The values of the fitting parameters are indicated in each figure part. The sensitivity for changing the r_0, a, and κ parameters can be recognized in (a), (b), and (c) of the figure, respectively.

TABLE I. Summary of fitting parameters for the investigated systems.

Donor-acceptor system	$\kappa r_C/D$	a (Å)	Initial e-h pair radius (Å)	MPL signal magnitude (%)
m-MTDATA:BPhen	1–10	9.4	27.1	0.43
m-MTDATA:BCP	0.1–1	9.4	23.4	0.24
2TNATA:BCP	10–100	9.4	20.6	0.10

For this purpose, however, the STNH formalism as a pertinent approach should be applied.

The corresponding magnetic field dependencies of MPL signals are plotted in Fig. 3. The figure shows that, independent of the D:A system, the MPL(B) characteristics consist of initial rises followed by flat regions, with the latter ones emerging for magnetic field intensities exceeding several milliteslas. Indeed, according to the EHP model, on this hyperfine scale of B-fields, the ISC is to be gradually switched off and the sample photoluminescence is expected to become magnetic-field insensitive. As far as the results of EML and MPL experiments are compared, a distinct correlation between the e-h pair intercarrier distance and the magnitude of the magnetic-field effect on photoluminescence of the given organic systems can be found (see Table I). In addition, the magnetic field effect on electroluminescence (MEL) in m-MTDATA systems showed a similar tendency;[6] however, the e-h pairs more loosely bound are involved in the electrical excitation regime. For comparison, the MPL effect as high as ca. 0.4% was observed in the thermally activated delayed fluorescence (TADF-type) m-MTDATA:t-Bu-PBD [2-(4-tert-Butylphenyl)-5-(4-biphenylyl)-1 ,3,4-oxadiazole] system. Note that the triplet back transfer to a lower-energy triplet exciton (the triplet drain) process that quenches the triplet charge transfer (CT) states occurs in that examined system. With no triplets drained, the MPL magnitude rises up to ca. 3.5% as observed in the m-MTDATA:3TPYMB (Tri[3-(3-pyridyl)mesityl]borane) mixture.[1,20]

Therefore, the e-h pairs, designated above as $(D^+ \ldots A^-)_{short}$, are involved in the processes of electro- and magnetomodulation photoluminescence of the D:A systems. Interestingly, the pairs of the short intercarrier distance do also produce the photoconductivity but with

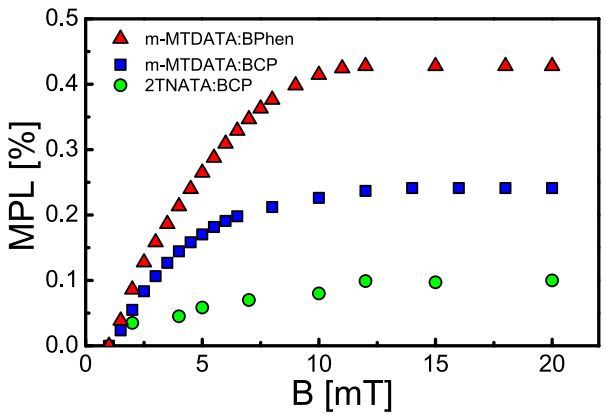

FIG. 3. The magnetic field dependencies of sample photoluminescence (the MPL signals) for three donor-acceptor systems. The circles are for the case of 2TNATA:BCP, the squares for m-MTDATA:BCP, and the triangles for the m-MTDATA:BPhen mixture.

the dominating contribution of the long-distanced pairs (cf. Ref. 24). The presence of long-radius pairs cannot be, however, detected during MPL measurements due to their nonradiative decay. Finally, it is worth noting that our measurements were carried out at weak magnetic fields where the EHP model is mainly relevant. At stronger fields, however, other mechanisms can be involved: the Δg mechanism (resulting from the difference between the values of giromagnetic Lande factors, g, of e-h pair components), as well as the triplet-charge (polaron) quenching Tq-mechanism (see Refs. 7 and 26), employing the proposed trion model (see, for example, Ref. 26).

To sum up, the electro- and magnetomodulation of photoluminescence of electron donor-acceptor systems made it possible to identify the e-h pairs involved in the process of exciton dissociation. The correlation between the pair radii and the magnitude of the magnetic-field effect on photoluminescence was identified, and the dissociation mechanism was found to proceed according to the EHP model, with the weak magnetic field modulating the intersystem crossing between the singlet, ^{1}(e-h), and triplet, ^{3}(e-h), pairs. The STNH-extension of the standard Onsager formalism was employed to investigate the pair dissociation process which allowed us to estimate the value of the final charge carrier recombination rate.

See the supplementary material for the details of the sample preparation and structure, fitting of the experimental data, and photocurrent characteristics of the systems.

REFERENCES

[1]T. Basel, D. Sun, S. Baniya, R. McLaughlin, H. Choi, O. Kwon, and Z. V. Vardeny, Adv. Electron. Mater. **2**, 1500248 (2016).
[2]C. L. Braun, J. Chem. Phys. **80**, 4157 (1984).
[3]A. I. Burshtein, J. Chem. Phys. **117**, 7640 (2002).
[4]W. Chang, D. N. Congreve, E. Hontz, M. E. Bahlke, D. P. McMahon, S. Reineke, T. C. Wu, V. Bulović, T. V. Voorhis, and M. A. Baldo, Nat. Commun. **6**, 6415 (2015).
[5]L. L. Chen, W. L. Li, M. T. Li, and B. Chu, J. Lumin. **122–123**, 667 (2007).
[6]P. Chen, Q. Peng, L. Yao, N. Gao, and F. Li, Appl. Phys. Lett. **102**, 063301 (2013).
[7]Y. Chen, W. Jia, J. Xiang, D. Yuan, Q. Chen, L. Chen, and Z. Xiong, Org. Electron. **39**, 207 (2016).
[8]C. Deibel, T. Strobel, and V. Dyakonov, Phys. Rev. Lett. **103**, 036402 (2009).
[9]K. Falkowski, W. Stampor, P. Grygiel, and W. Tomaszewicz, Chem. Phys. **392**, 122 (2012).
[10]E. Frankevich, A. Zakhidov, K. Yoshino, Y. Maruyama, and K. Yakushi, Phys. Rev. B **53**, 4498 (1996).
[11]H. Hayashi, *Introduction to Dynamic Spin Chemistry* (World Scientific, Singapore, 2005).
[12]J. Kalinowski, *Organic Light Emitting Diodes: Principles, Characteristics, and Processes* (Marcel Dekker, New York, 2005).
[13]J. Kalinowski, M. Cocchi, D. Virgili, V. Fattori, and J. A. G. Williams, Chem. Phys. Lett. **432**, 110 (2006).
[14]J. Kalinowski, M. Cocchi, D. Virgili, P. D. Marco, and V. Fattori, Chem. Phys. Lett. **380**, 710 (2003).
[15]J. Kalinowski, W. Stampor, M. Cocchi, D. Virgili, and V. Fattori, Appl. Phys. Lett. **86**, 241106 (2005).
[16]J. Kalinowski, W. Stampor, and P. D. Marco, J. Chem. Phys. **96**, 4136 (1992).
[17]J. Kalinowski, J. Szmytkowski, and W. Stampor, Chem. Phys. Lett. **378**, 380 (2003).
[18]A. Köhler and H. Bässler, *Electronic Processes in Organic Semiconductors: An Introduction* (Willey-VCH, Weinheim, 2015).
[19]L. J. A. Koster, E. C. P. Smits, V. D. Mihailetchi, and P. W. M. Blom, Phys. Rev. B **72**, 085205 (2005).
[20]Y. Lei, Q. Zhang, L. Chen, Y. Ling, P. Chen, Q. Song, and Z. Xiong, Adv. Opt. Mater. **4**, 694 (2016).
[21]J. Noolandi and K. M. Hong, J. Chem. Phys. **70**, 3230 (1979).
[22]N. Ohta, S. Umeuchi, Y. Nishimura, and I. Yamazaki, J. Phys. Chem. **102**, 3784 (1998).
[23]L. Onsager, Phys. Rev. **54**, 554 (1938).
[24]D. Pelczarski, P. Grygiel, K. Falkowski, M. Klein, and W. Stampor, Org. Electron. **25**, 362 (2015).
[25]H. Sano and M. Tachiya, J. Chem. Phys. **71**, 1276 (1979).
[26]A. J. Schellekens, W. Wagemans, S. P. Kersten, P. A. Bobbert, and B. Koopmans, Phys. Rev. B **84**, 075204 (2011).
[27]Y. Sheng, T. D. Nguen, G. Veeraraghavan, Ö. Mermer, M. Wohlgenannt, S. Qiu, and U. Sherf, Phys. Rev. B **74**, 045213 (2006).
[28]A. Weller, H. Staerk, and R. Treichel, Faraday Discuss. Chem. Soc. **78**, 271 (1984).